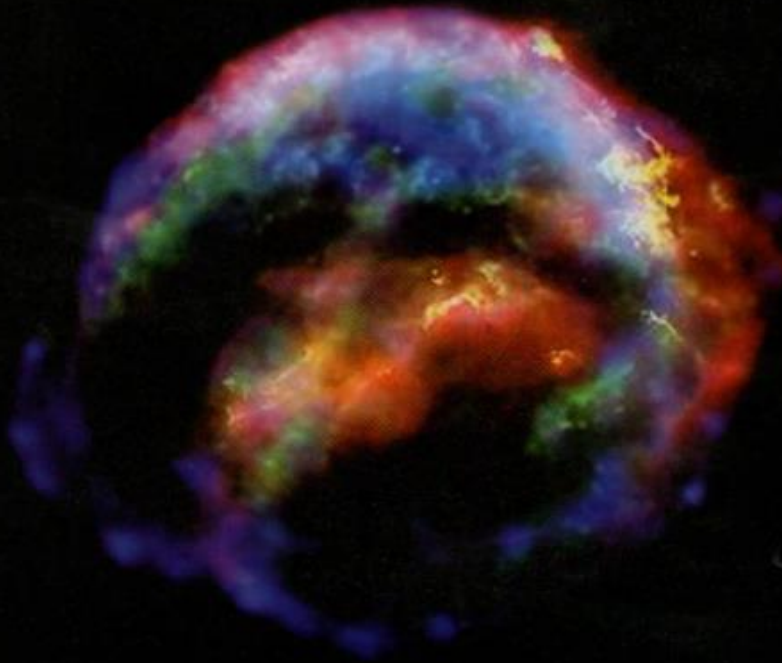


**International Journal of  
Mechanical & Mechatronics  
Engineering**

**ISSN # 2077 - 124X**



I

J

M

M

E



**IJENS Publishers  
International Journals of  
Engineering n Sciences**

## IJMME - IJENS Editorial Board

### Chief Editor IJMME IJENS

Name and Picture	Major Areas of Interest	Current Address	Details
 Talal K. Kassem	Renewable Energy – Thermal Power Engineering	Mechanical Engineering Dept. Taif University P. O. Box 888, Zip Code 21974 Taif - Al - Haweiah	<a href="#">IJENS-1035-Kassem</a>

### INSTRUCTION

For paper submission, kindly use Online Submission and to contact use [ijmme@ijens.org](mailto:ijmme@ijens.org) or [editor@ijens.org](mailto:editor@ijens.org) or [editor.ijens@gmail.com](mailto:editor.ijens@gmail.com)

### Editors IJMME IJENS

Name and Picture	Major Areas of Interest	Current Address	Details
 Ali Sadq Yasir	Mechanical Engineering, Applied Mechanics	Engineering Faculty, Kufa University, Iraq	<a href="#">IJENS-1005-Sadq</a>
 Ayman A. Aly	Mechatronics-Automatic control	Taif University	<a href="#">IJENS-1033-Aym</a>
 Mohd Afendi	Fracture Mechanics, Adhesive Joint, Friction Stir Welding, Finite Element Method, Renewable Energy	School of Mechatronic Engineering, Universiti Malaysia Perlis (UniMAP), Pauh Putra Campus, 02600 Arau, Perlis, Malaysia	<a href="#">IJENS-1049-Afendi</a>
 Sivarao Subramonian	Advanced materials processing, Advanced machining, Artificial Intelligence in manufacturing, Innovative system engineering	Faculty of manufacturing Engineering, Universiti Teknikal Malaysia Melaka, 76100 Durian Tunggal, Melaka, Malaysia	<a href="#">IJENS-1038-Sivarao</a>
 Peng-Sheng Wei	Applications of electron and laser beam, plasma, and resistance welding through theoretical analyses coupled with verification experiments	Dept. Mechanical and Electro-Mechanical Engineering, National Sun Yat-Sen University, Kaohsiung, Taiwan, ROC	<a href="#">IJENS-1043-Wei</a>
 BOCI SEVASTIAN LIVIU	Classic and high speed railway vehicles (Braking systems, Traction systems	RO-310068 ARAD, Clujului Street, no. 81, Bloc 81, Scara A, Apt. 3	<a href="#">IJENS-1046-Bocli</a>

## Tim Penelaah

- Prof. Dr. Adlim, M.Sc (Universitas Syiah Kuala, Indonesia)
- Drs. Mahyuddin K.M. Nasution, M.IT, Ph.D (Universitas Sumatera Utara, Indonesia)
- Prof. Saib Suwilo, M.Sc, Ph.D (Universitas Sumatera Utara, Indonesia)
- Prof. Basuki Wirjosentono, M.S, Ph.D (Universitas Sumatera Utara, Indonesia)
- Prof. Dr. Erman Munir, M.Sc (Universitas Sumatera Utara, Indonesia)
- Prof. Dr. Syafruddin Ilyas, M.Biomed (Universitas Sumatera Utara, Indonesia)
- Prof. Timbangan Sembiring, M.Sc (Universitas Sumatera Utara, Indonesia)
- Prof. Tulus, M.Si (Universitas Sumatera Utara, Indonesia)
- Prof. Dr. Jamaran Kaban, M.Sc (Universitas Sumatera Utara, Indonesia)
- Dr. Ir. Iman Rusmana, M.Si (Institut Pertanian Bogor, Indonesia)
- Dr. Iwantono, M.Phil (Universitas Riau, Indonesia)
- Saharman Gea, Ph.D (Universitas Sumatera Utara, Indonesia)
- Dr. Elvina Herawati, M.Si (Universitas Sumatera Utara, Indonesia)
- Dr. Eng. Himsar Ambarita, S.T, M.T (Universitas Sumatera Utara, Indonesia)
- Dr. Irwana Nainggolan (Universitas Sumatera Utara, Indonesia)
- Dr. Salomo Hutahaeen, M.Si (Universitas Sumatera Utara, Indonesia)
- Dr. Etti Sartina Siregar, M.Si (Universitas Sumatera Utara, Indonesia)
- Dr. Isnaini Nurwahyuni, M.Sc (Universitas Sumatera Utara, Indonesia)
- Dr. Kiki Nurtjahja, M.Sc (Universitas Sumatera Utara, Indonesia)
- Dr. Syahrul Humaidi, M.Sc (Universitas Sumatera Utara, Indonesia)
- Dr. Suyanto, M.Kom (Universitas Sumatera Utara, Indonesia)

# Study on the Characteristics of a Natural Vacuum Desalination System Using Solar Energy as Energy Sources

EkoYohanes Setyawan<sup>1</sup>, Farel H Napitupulu<sup>2</sup>, HimsarAmbarita<sup>2,3\*</sup>

<sup>1</sup>Mechanical Engineering Department, National Institute of Technology Malang, Indonesia

<sup>2</sup>Sustainable Energy and Biomaterial Centre of Excellent, Faculty of Engineering, University of Sumatera Utara, Jl. Almamater Kampus USU Medan 20155, Indonesia

<sup>3</sup>Mechanical Engineering, University of Sumatera Utara, Jl. Almamater Kampus USU Medan 20155, Indonesia

\*Correspondence: [himsar@usu.ac.id](mailto:himsar@usu.ac.id)

**Abstract**— The characteristics of a natural vacuum solar desalination unit is studied. A prototype of natural vacuum solar desalination consists of solar collector, evaporator and condenser as the main components has been designed and fabricated. The collected heat in the 3 m<sup>2</sup> solar collector is transferred into the evaporator using a transfer fluid system flowed by a pump powered by solar cell. The objective is to explore the characteristics of fresh water production of the natural vacuum solar desalination. The prototype is tested by exposing the unit to solar irradiance on a top roof of a building in Medan city of Indonesia. The experiments are carried out from 8.00 WIB to 16.00 WIB local time. The results show that the prototype can produce fresh water from 0.87 liters to 1.47 liters per day. The characteristics of fresh water production rate can be divided into five different periods. The first period is initial period or the period without fresh water production. The second period is first rising rate, where the main driving force for desalination is solar irradiation. The third period is constant production rate. The fourth period is second rising production rate, where the main driving force for desalination is ambient temperature. And the final period is falling production rate. The thermal efficiency of the system is relatively low which varies between 6.95% and 8.69%. Those facts suggest that the present prototype is far from efficient. Thus, several modifications are needed to improve the performance of the system.

**Index Term**— Solar Energy; Desalination; Natural Vacuum; Seawater

## I. INTRODUCTION

Industrialization, life standard and depletion of natural resources make the demand of fresh water increasing significantly. United Nation Organization predicts that by the year of 2025, almost 1800 million people around the world will be under terrible water scarcity [1]. The most potential solution to this problem is desalination of seawater technologies. The desalination system is not a new technology for human being. Nowadays, desalinations have been done in many regions of the world to meet their need on fresh water. Those include countries in the Middle East, Arabic countries, North America, some of Asian countries, Europe, Africa, Central America, South America and Australia [2]. Several

methodologies of desalination such as multi-stage flash, multi-effects distillation, vapor compression, reversal osmosis, and electro-dialysis are already available in practical uses. The conventional desalination systems that now in services are mainly powered by fossil fuel. Kalogirou reported that about 10,000 ton of fossil fuel is burned to power desalination systems in the world in a year [3].

Those facts motivate researchers to carry out research on sustainable desalination systems. The sustainable desalination system must meet the need for using fossil fuel more efficient or can be powered by renewable energy resources or waste heat [4]. The renewable energy resources that commonly used to power desalination system are solar energy, wind power, and geothermal energy. Among those, solar energy is the most used. According to study by Eltawil et al., it is up to 57%. It is predicted that, desalination system powered by solar energy, here after named as solar desalination, will be more popular in the future. In order to develop the sustainable desalination systems, even the countries that known biggest fossil fuel producers such as Saudi Arabia are enhancing the use of solar energy to power their desalination systems. The innovations on desalination system powered by renewable energies and waste heat have been reported by several researchers. Gude et al. reported a feasibility study of a new two-stage low temperature desalination [5]. The results revealed that the two-stages desalination process has potential for standalone small to large scale applications in water and energy scarce rural areas. It was revealed that the specific energy consumption of the system was 15000 kJ/kg of fresh water. The cost will be less than \$ 7 per m<sup>3</sup> fresh water, if it is operated by solar energy. A system that combines multi effect distillation desalination with a supercritical organic Rankine Cycle and an ejector has been proposed by Li et al.[6]. The proposed system works like a combined heat, power and condensation. The thermal performance of the system was analyzed theoretically using an engineering equation solver program. The results revealed that the overall exergy efficiency close to 40% for salt concentration of 35 g/kg using a low temperature heat source of 150°C.

An exergy analytical study on the performance of a new combined vacuum desalination and power system as a heat

recovery reported by Araghi et al. [7]. The system was claimed can be operated on waste heat and an organic working fluid. The results showed that the overall performance of the introduced system was comparable with the discharge thermal energy combined desalination system utilizing ammonia mixture. However in term of desalination, the proposed system produces more fresh water. An experimental study on water separation process in a lab scale novel spray flash vacuum evaporator by using a heat-pipe (HP) reported by Gao et al. [8]. Cold source and heat source temperatures, spray temperature, and spray flow are used in the parametric studies. On the evaporator bland plate, a maximum heat flux density of  $32 \text{ W/cm}^2$  can be achieved. The heat-pipe absorbs energy effectively from low grade heat source then transfer the energy to the droplets already flashed, so as to maintain or even increase the superheat degree of droplets during the evaporation process. Fresh water yield was affected by the heat source temperature. The higher heat source temperature is the more heat that droplets can obtain and the faster evaporation process will be. Another important factor of fresh water yield is cooling water temperature. Experimental study on a pilot plant of direct contact membrane distillation (DCMD) driven by low grade waste heat: membrane fouling and energy assessment reported by Dow et al.[9]. The pilot desalination unit was located at a gas fired power station which provided the heat source with temperature lower than  $40^\circ\text{C}$  and waste water to the DCMD system with  $0.67 \text{ m}^2$  of membrane area. Based on the available energy for a continuously operating 500 MW (electric power) rated power station, the treatment potential was estimated at up to 8000 kilo liter/day.

Study on the comparison of a boosted multi-effect distillation (MED) for sensible low-grade heat source with feed pre-heating multi-effect distillation has been reported by Christ et al. [10]. It was revealed that for most operational conditions germane to sensible waste heat source and renewable energies, the boosted MED system offers both thermodynamic and economic superior performances, especially when low heating media temperatures prevail. Gude et al. [11] reviewed the energy storage options for different desalination technologies using various renewable energy and waste heat source. The focus of the review was on the thermal energy storage system. Bundschuh et al. [12] evaluated the potency and suitability of different types and low-cost low-enthalpy ( $50\text{-}150^\circ\text{C}$ ) geothermal heat sources for water desalination. It was suggested that geothermal option is superior to the solar option if low-cost geothermal option is available because it provides a constant heat source in contrast to solar. Cicolanti et al. [13] compared different operation modes of a single effect thermal desalination plant using waste heat from micro Combined Heat and Power experimentally. The plant can be operated both in batch and in continuous operation modes. The desalination unit consists of a 1 kW Stirling engine coupled with a single effect thermal desalination plant for the simultaneous production of electricity and  $> 150 \text{ L/day}$  of fresh water.

Those studies are focused on the multi-effect distillation and the combination with power system. Another interesting

method that can be used in the desalination system is natural vacuum desalination. Several studies on natural vacuum desalination system have been found in literature. In the system the seawater is placed in a container which is vacuumed naturally by using the gravity of the water. The vacuum system advantage is that a low grade heat source such as solar energy can be used efficiently. The research on preliminary experimental and theoretical analysis of a natural vacuum water desalination system using low-grade solar heat has been reported by Al-Kharabsheh and Goswami [14]. The effects of several various operating conditions were investigated. The simulation in Gainesville, Florida showed that the daily output from a system of  $1 \text{ m}^2$  of evaporator area with  $1 \text{ m}^2$  of solar collector area could reach 6.5 kg of fresh water. A study on vacuum desalination system coupled with solar collector of  $18 \text{ m}^2$  and thermal energy storage with a volume of  $3 \text{ m}^3$  was reported by Gude et al.[15]. The proposed desalination unit is capable of producing 100 L/day fresh water. Gude and Nirmalakandan [5] use the same solar desalination system and combined it with a solar-assisted air-conditioning system. The results showed that cooling capacity of 3.25 kW and distillate yield of 4.5 kg/hour can be obtained. The modified natural vacuum with flash desalination system operation using in single stage mode and two stage mode has also been investigated [16]. With a solar collector of  $1 \text{ m}^2$  area, the proposed system produces nearly 5.54 kg and 8.66 kg of distillate while operating in single stage and two stage modes with a performance ratio of 0.748 and 1.35, respectively. A natural vacuum desalination that consists of evaporator column exposed to solar radiation and shaded condenser column has been proposed by Ayhan and Al-Madani [17]. Here a vapor from evaporator to condenser was moved by the blower. Ambarita [18] employed an electric heater to simulate solar energy at a constant temperature heat source in a natural vacuum desalination unit. Ambarita et al. reported a simulation study on a natural vacuum desalination unit with variable heat source of the same system as in the previous study. Recently, Setyawan et al. [19] modified the form of the evaporator into square form and reported a preliminary field test of a natural vacuum solar desalination unit. In addition, the evaporator was not insulated. Thus, the fresh water production was very low.

Those reviewed studies showed that investigation of natural vacuum solar desalination system has come under scrutiny. However, focus of those studies lies on the performance of the natural vacuum solar desalination system where the heat supply unit was replaced by artificial solar energy. In addition, research methodology used in those studies is numerical approach. In other words, study on the natural vacuum solar desalination unit tested in the real field by exposing directly to the sun is very limited. In this paper, the performance of a natural vacuum solar desalination is studied experimentally. Here, the natural vacuum desalination unit is tested in the real condition by exposing it to solar irradiance. The main objective is to explore the operational characteristics of the natural vacuum desalination system when it is exposed to the solar irradiation. The tests are carried out for several sunny days. The results of the present study are expected to supply

the necessary information in the developing high performance solar desalination system.

## II. EXPERIMENTAL APPARATUS AND METHODS

In this study, numerical and experimental works are carried out. A prototype of natural vacuum solar desalination unit has been designed and fabricated. Figure 1 shows the schematic diagram and photograph of the system. It consists of evaporator, condenser, seawater tank, fresh water tank, saline water tank, and solar collector. The evaporator is made of cylindrical stainless steel 304 with diameter, height and thickness of 0.8 m, 20 cm, and 5 mm, respectively. The upper part of the evaporator covered with conical with height of 40 cm. In order to decrease the heat loss to the ambient, the evaporator covered by insulation made of rockwool with thickness of 5 cm. The heat from solar collector is injected into the evaporator by using transfer fluid flows inside a heating coil tube. It is made of copper with diameter and length of 2.1 cm and 2.4 m, respectively.

The condenser of the system is a heat exchanger made of stainless steel 304. It is a horizontal circular tube with circular fins with a thickness of 2.54 mm. The inside diameter and the length of the condenser is 100 mm and 500 mm, respectively. The number of fin is 10 fins with a diameter and thickness of 254 mm and 0.6 mm, respectively. The space between fins is 40 mm. The condenser and the evaporator are connected by using a flange with a diameter and thickness of 128 mm and 15 mm, respectively. The used solar collector is flat plate type with double glass covers. It consists of two similar solar collectors arrange in series. The dimension of each collector is 1 m of wide and 1.5 m of length. Thus, the total collector area is 3 m<sup>2</sup>. In this study, water is used as a transfer fluid to transfer the heat from the solar collector to the evaporator. As a note, the specific different of the present natural vacuum desalination is the use of photovoltaic to power a pump. The pump is employed to flow the transfer fluid in order to bring the heat from solar collector to the evaporator. In this study, the maximum power and collector area of the photovoltaic are 100 Wp and 1196 mm × 541 mm, respectively. In order to provide heat recovery, the pipe where fresh water flows in to evaporator and the pipe where the brine drawn from the evaporator connected to an annular type heat exchanger as shown in the schematic diagram of Figure 1.

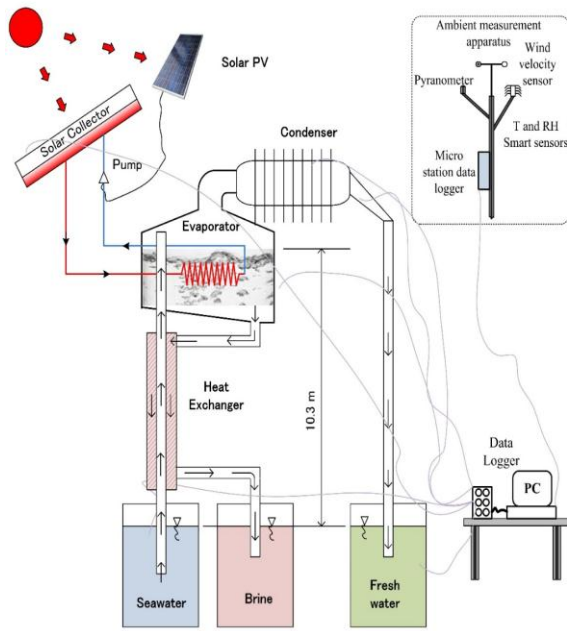
In every experiment, at the beginning, the system must be vacuumed. Firstly, all of the components of the system (evaporator, tube-in-tube heat exchanger and condenser) are filled with seawater. As a note, the evaporator, condenser and solar collector of the system are located at a position 10.3 m above the seawater, brine and fresh water tanks. To create the vacuum in the system, each valve in the feeder pipes (pipe in the heat exchanger) is opened. Thus, the seawater in the evaporator will fall down due to the gravitational force. As a result, a vacuum chamber in the evaporator will be present. Thus, the experiment can be started.

The process of vacuum desalination in the system can be explained as follows. The solar collectors absorb the solar irradiation and the temperature increasing. This heats the

transfer fluid inside the pipe. At the same time, photovoltaic receives the solar irradiation and converts it into electricity. The resulted electricity is used to powers the pump and it circulates the transfer fluid. Thus, the heated transfer fluid in the solar collectors is flowed into the evaporator by the pump. In the evaporator, the hot transfer fluid will heat the seawater in the evaporator. As a result, the seawater temperature in the evaporator will increase. Since the pressure in the evaporator is below the atmosphere or below the saturation pressure, the fresh water will evaporate from the seawater a rate of  $\dot{V}_e$  [m<sup>3</sup>/s]. The resulted vapor will naturally flow to the condenser. Since the temperature of the condenser wall is lower, the vapor will be condensed in the condenser. This results in fresh water as the main product. The evaporation process makes salinity of seawater in the evaporator increases. The increasing salinity of seawater will decrease the evaporation rate in the evaporator or the freshwater production rate will be dropped. To avoid this, the high concentration of saline water in the evaporator (brine water) is withdrawn with a rate of  $\dot{V}_w$  [m<sup>3</sup>/s]. The flow out of the brine from the evaporator makes the pressure in the evaporator close to vacuum. Since the pressure in the evaporator close to vacuum, the seawater in the tank will be drawn and flows into the evaporator. The volume rate of the seawater flow into the evaporator is  $\dot{V}_i$  [m<sup>3</sup>/s].



(a) Photograph of Experimental Set up



(b) Diagram of Experimental Set up

Fig. 1. The photograph and schematic diagram of the natural vacuum desalination system

In order to provide data for analysis, two data acquisition systems are also designed and installed to the experimental apparatus. The first datalogger is a multi-channel Agilent 34972, it is employed to record temperatures with an interval of 1 minute. Temperatures on the system are measured by using *J*-type thermocouples with uncertainty equal to 0.1°C. There are 20 thermocouples are used. Those thermocouples are placed as follows: four thermocouples placed in the evaporator, four in the condenser, four in the heat exchanger and the rests in pipe and water containers. The second datalogger is HOBO micro station which is utilized to record weather condition during experiments. Solar radiation is measured using HOBO pyranometer smart sensor. The ambient temperature and relative humidity (RH) are measured using HOBO temperature RH smart sensor with an accuracy of 0.2°C and ± 2.5% RH, respectively. The wind speed around the experimental apparatus is measured with HOBO wind speed smart sensor with accuracy ± 1.1 m/s.

### 2.1 Analysis of the natural vacuum desalination

In order to examine the evaporation rate in the evaporator, temperature of the seawater inside the evaporator is needed. In the experiment, it is difficult to install measurement apparatus to measure seawater temperature inside the evaporator. In the present experiment, there is no measurement apparatus is used to measure the temperature of the seawater in the evaporator. To overcome the absence of the inner temperature of the seawater in the evaporator, numerical method is developed. In the numerical method, the governing equations are developed as follows. In the evaporator, the mass conservation leads to:

$$\frac{d}{dt}(\rho V)_s = \rho_i \dot{V}_i - \rho_w \dot{V}_w - \rho_e \dot{V}_e \quad (1)$$

Where  $V$  [m<sup>3</sup>] and  $\rho$  [kg/m<sup>3</sup>] is the volume and density of the seawater in the evaporator, respectively. The subscripts of  $s$ ,  $i$ , and  $e$  stand for seawater, injected, and evaporation, respectively. The saline conservation in the evaporator can be written in the following equation:

$$\frac{d}{dt}(\rho C V)_s = (\rho C)_i \dot{V}_i - (\rho C)_s \dot{V}_w \quad (2)$$

In the above equation,  $C$  [%] is the solute concentration. If the temperature of the sea water in the evaporator is assumed to be uniform, the conservation of energy yield to equation (3).

$$\frac{d}{dt}(\rho c_p V T)_s = \dot{Q}_m + (\rho c_p T)_i \dot{V}_i - (\rho c_p T)_s \dot{V}_w - \dot{Q}_e - \dot{Q}_{wall} \quad (3)$$

where,  $\dot{Q}_{in}$  [Watt] and  $c_p$  [J/kgK] is the heat transfer rate from heater and specific heat capacity, respectively.

As mentioned in the previous section, the solar energy from the solar collector is transferred to the evaporator using water as a transfer fluid. The transfer fluid is flowed inside pipe. In the evaporator, the pipe is submerged in the seawater horizontally. The mechanism of heat transfer between the transfer fluid and seawater in the evaporator can be divided into forced convection inside the pipe, conduction in the pipe wall and natural convection on the outer surface. Since the thermal resistance on the outer surface is way bigger than thermal resistance on the inner surface and the wall, it is assumed that the temperature of the pipe wall and transfer fluid is similar. Thus, only the natural convection on the outer surface of the pipe is taken into account. Thus, the heat input from the fluid in the pipe to the seawater in the evaporator can be calculated using the following equation.

$$\dot{Q}_i = Nu_{sur} \frac{k_s}{D_h} A_{sur} (T_{sur} - T_s) \quad (4)$$

where  $D_h$  [m],  $A_{sur}$ ,  $Nu_{sur}$ , and  $T_{sur}$  is the diameter, surface area, Nusselt number, and surface temperature of the heater, respectively.

The following equations are used to determine the energy needed for evaporation the seawater in the evaporator.

$$\dot{Q}_e = \rho \dot{V}_e h_{fg} \quad (5)$$

Where  $\square_{fg}$  [J/kg] is the latent heat evaporation of the seawater. In the present study, the evaporator is divided into bottom, side wall and top wall. Heat capacity of evaporator materials is taken into account. The energy conservation in the bottom plate of the evaporator gives:

$$\frac{\partial}{\partial t} (\rho c_p T)_b = \frac{Nu_{b,i}}{L_b} k_s (T_s - T_b) - \frac{Nu_{b,o}}{L_b} k_a (T_s - T_a) \quad (6)$$

where the subscript  $b$  and  $a$  refer to bottom of the evaporator and ambient air, respectively. While, the subscript  $i$  and  $o$  refer to inside and outside surfaces of the evaporator, respectively. And  $L$  is the characteristic length of the surface. The Nusselt numbers on the inside surface ( $Nu_{b,i}$ ) and outside ( $Nu_{b,o}$ ) are calculated by equation proposed by Incropera et al. (2006) and Lloyd and Sparrow (1970), respectively.

The following equations are used to determine energy conservation to the side walls:

$$\frac{\partial}{\partial t} (\rho c_p VT)_d = \frac{Nu_{d,i}}{L_d} k_s (T_s - T_d) - \frac{Nu_{d,o}}{L_d} k_a (T_s - T_a) \quad (7)$$

where the subscript  $d$  refers to side wall of the evaporator. The parameter  $Nu_{d,o}$  is the Nusselt number on outer surface of the wall. Application of energy conservation to the top wall of the evaporator gives:

$$\frac{\partial}{\partial t} (\rho c_p VT)_t = \frac{Nu_{t,i}}{L_t} k_v (T_s - T_t) - \frac{Nu_{t,o}}{L_t} k_a (T_s - T_a) \quad (8)$$

where the subscript  $t$  refers to top wall. As a note, the fluid in the inside of the top wall is water vapor (shown by subscript  $v$ ) at a pressure close to vacuum.

In the condenser analysis, several assumptions are made. It is assumed all of vapor at temperature of  $T_s$  is condensed into fresh water at temperature  $T_f$  which is equal to condenser inside temperature of the ( $T_{c,i}$ ). The inside temperature of the condenser is strongly affected by ambient temperature. The application of energy conservation gives the following equation.

$$(\rho \dot{V})_e h_{fg}^* = \frac{2\pi d_c k_c (T_f - T_{c,o})}{\ln(r_{c,o}/r_{c,i})} \quad (9)$$

where the subscript  $c$  refers to condenser and  $r$  is the radius of the condenser. The modified latent heat of condensation  $\square_{fg}^*$  [J/kg] is given by Rohsenow et al. (1985).

$$h_{fg}^* = h_{fg} + 0.68 c_{pf} (T_s - T_f) \quad (10)$$

To calculate the temperature of the outer surface of the condenser heat transfer rate is used from the condenser surface

$$\dot{Q}_c = [h_{co,tip} NA_{f,tip} \eta_f + h_{co} NA_{f,sides} \eta_f + h_{co} A_{base}] (T_{co} - T_a) \quad (11)$$

Where  $\dot{Q}_c$  is heat transfer rate from the condenser. The subscript  $f$ ,  $tip$ , and  $base$  refer to fin, tip surface, and base surface of the condenser.

In the heat exchanger, the feed seawater is heated before entering the evaporator. Temperature of the seawater entering the evaporator is given by:

$$T_i = T_0 + \frac{\varepsilon (\rho \dot{V} c_p)_{\min} (T_s - T_0)}{\rho_0 \dot{V}_i c_{p0}} \quad (12)$$

where the subscript 0 and min refer to initial condition of the seawater and minimum value of heat capacity of the fluid stream, respectively.

The following equation is used to calculate the rate of evaporation between two places where one contains seawater and other fresh water (Bemporad, 1995).

$$\dot{V}_e = A_{sur} \frac{\alpha_m}{\rho_f} \left[ f(C_s) \frac{P(T_s)}{(T_s + 273)^{0.5}} - \frac{P(T_f)}{(T_f + 273)^{0.5}} \right] \quad (13)$$

Where  $\dot{V}_e$  [m<sup>3</sup>/s] and  $A_{sur}$  [m<sup>2</sup>] is volume evaporation rate and evaporation surface. The parameter  $\alpha_m$  [kg/m<sup>2</sup>.Pa.s.K<sup>0.5</sup>] is an empirical coefficient which is developed from experiments. Al-Kharabsheh and Goswani (2004) suggested the following value.

$$10^{-7} \leq \alpha_m \leq 10^{-6} \quad (14)$$

Several experimental data and calculations have been made to determine an appropriate value of  $\alpha_m$ . The value of  $\alpha_m = 9 \times 10^{-9}$  is suitable for the present experiments and simulation. Thus, this value will be used for all simulations (Ambarita, 2016). Vapor pressure  $P$  [Pa] as a function of temperature is given by Al-Kharabsheh and Goswani (2003) :

$$P(T) = 100 \times \exp[63.042 - 7139.6/(T + 273) - 6.2558 \ln(T + 273)] \quad (15)$$

The correction factor of  $f(C)$  is calculated using the following equation:

$$f(C) = 1 - 0.0054C \quad (16)$$

## 2.2. Solar Irradiance

In order to provide theoretical solar irradiance, numerical analysis is also developed. The total heat collected from the solar radiation is calculated by equation below.

$$Q_{rad} = \int_{tsr}^{tss} I dt \quad (17)$$

where  $tsr$  and  $tss$  are time at sunrise and time at sunset at the solar collector, respectively. Solar irradiance  $I$  [W/m<sup>2</sup>] is the data collected from measurement of HOBO micro station data logger. The following equation is used to calculate the clear sky radiation at the location.

$$G_{tot} = G_{on} \cos \theta_z [\tau_b + 0,271 - 0,294\tau_b] \quad (18)$$

where  $G_{on}$ ,  $\theta_z$ , and  $\tau_b$  are extraterrestrial radiation, zenith angle, and the atmospheric transmittance for beam radiation, respectively. The zenith angle is given by the following equation:

$$\cos \theta_z = \cos \phi \cos \delta \cos \omega + \sin \phi \sin \delta \quad (19)$$

where  $\phi = 3^\circ 34'$  is used as the latitude in at Medan city,  $\delta$  is declination angle depends on the day of experiment, and  $\omega$  is hour angle. The declination angle is calculated using the following equation.

$$\delta = 23,45 \sin \left( 360 \frac{284+n}{365} \right) \quad (20)$$

where  $n$  is the number of day. The hour angle is calculated by:

$$\omega = 15(STD - 12) + (ST - STD) \times \frac{15}{60} \quad (21)$$

where  $STD$  and  $ST$  are the standard time and solar time, respectively. The solar time is calculated by:

$$ST = STD - 4(L_{st} - L_{loc}) + E \quad (22)$$

where  $L_{st}$  is the standard meridian for the local time zone of Medan and  $L_{loc}$  is longitude of the location. The parameter  $E$  is the equation of time and it is calculated by the following equation.

$$E = 229,2(0,000075 + 0,001868 \cos B - 0,032077 \sin B - 0,014615 \cos 2B - 0,04089 \sin 2B) \quad (23)$$

and  $B$  is given by

$$B = (n - 1) \frac{360}{365} \quad (24)$$

The atmospheric transmittance for beam radiation is given by:

$$\tau_b = a_0 + a_1 \exp \left( \frac{-k}{\cos \theta_z} \right) \quad (25)$$

For Medan city, the constants in the above equation are calculated using the following equations.

$$a_0 = 0,95(0,4237 - 0,00821(6 - A)^2) \quad (26)$$

$$a_1 = 0,98(0,5055 + 0,00595(6,5 - A)^2) \quad (27)$$

$$k = 1,02(0,2711 + 0,01858(2,5 - A)^2) \quad (28)$$

The experiments are carried out at altitude of  $A = 0,02$  km.

In this study, the effect of temperature and concentration of solute to the seawater properties are taken into account. The nature of fluid transport is treated as a function of temperature

and for seawater. The equations suggested by Sharqawy et al. (2010) are used to calculate transport properties of seawater. The density of sea water is calculated by equations (Bromley et al. 1970).

### 2.3. Performance parameters

In this study, the performance is examined using two parameters. The first parameter is the amount of fresh water produced calculated by using the following equation, with the goal of natural vacuum desalination is to produce fresh water by using energy efficiently in the performance of the system used.

$$V_{tot} = \int_0^{t_{end}} \dot{V}_e dt \quad (29)$$

where  $\dot{V}_{tot}$  [m<sup>3</sup>] and  $t_{end}$  [s] is the total volume of the fresh water produced and time at the end of experiment/calculation. The thermal efficiency defined as the ratio of energy useful to the energy input is used in the second parameter.

$$\eta_{th} = \frac{Q_{useful}}{Q_{in}} = \frac{\int_0^t \rho \dot{V}_e h_{fg} dt}{\int_0^t \dot{Q}_{in} dt} \quad (30)$$

## III. RESULTS AND DISCUSSIONS

In this study, the experiments have been carried out in Mechanical Engineering building, Universitas Sumatera Utara, at Medan city of Indonesia. The location of the experiment is at coordinate  $3^\circ 34'$  North and  $98^\circ 40'$  East. The experiments have done during July 2017. Here, five days of experiments are discussed. Every experiment starts from 8.00 WIB and finishes at 16.00 WIB. Here, WIB is the local time in the experimental place.

### 1.1 Solar Irradiance

Figure 2 shows solar irradiance during experiments. In the figure, both measurement and clear sky irradiances are presented. The measured solar irradiance is shown by blue circle marks and the clear sky radiation shown by red line. In the first day of experiment, shown in Figure 2a, the measurements are far below the clear sky radiation. This fact reveals that in the first day of experiment the weather condition was cloudy. Even though the sky was cloudy, it can be seen that by noon, the solar irradiance increases as time increasing. In the afternoon, the solar irradiance decreases with increasing time. The measurement shows that, the minimum, maximum, and averaged solar irradiances are  $100.6 \text{ W/m}^2$ ,  $712.9 \text{ W/m}^2$ , and  $304.79 \text{ W/m}^2$ , respectively. By using equation (17), the total solar energy collected in the solar collector during the first day of experiment is 26.4 MJ. The second day of experiment shows a better solar irradiance. In the second day of experiment, solar irradiance is quite close to theoretical clear sky radiation. The minimum, maximum, and

averaged solar irradiances are  $111.9 \text{ W/m}^2$ ,  $759.4 \text{ W/m}^2$ , and  $452.01 \text{ W/m}^2$ , respectively. In addition, the total collected solar energy was  $39.73 \text{ MJ}$ . This fact shows that the solar irradiance of the second day is better than the first day.

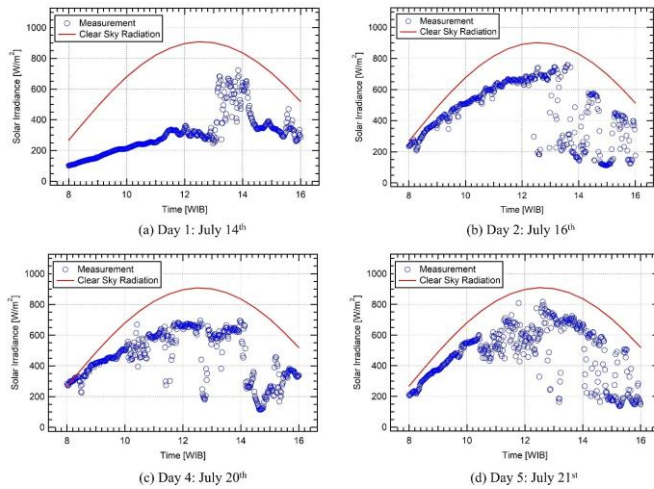


Fig. 2. Solar Irradiance during experiments

The characteristics of solar irradiance during five days of experiment are shown in Table 1. The table shows the minimum, maximum and averaged solar irradiances. Total collected solar energy by the solar collector is also shown in the table. The solar energy varies from  $26.40 \text{ MJ}$  to  $39.84 \text{ MJ}$ . The first day shows the lowest collected solar energy and the fourth day shows the highest.

Table 1 Characteristics solar irradiance during experiments

Day of Experiment	Solar Irradiance [ $\text{W/m}^2$ ]			Energy total [MJ]
	Min	Max	Averaged	
Day 1	100.6	721.9	304.97	26.40
Day 2	111.9	759.4	452.01	39.72
Day 3	134.4	724.4	426.72	36.93
Day 4	114.4	695.6	460.16	39.84
Day 5	190.6	795.6	454.38	39.33

### 1.2 Solar Collector

The solar irradiance heats the plate of the solar collector and the heat energy from the plate is transferred into the transfer fluid inside the pipe. Figure 3 shows temperatures history on the solar collector. They are temperature of the collector plate, temperature of the transfer fluid entering the collector, temperature of the fluid leaving from the collector and temperature of the top cover. The figure shows that the maximum temperature on the collector plate can reach a value over than  $100^\circ\text{C}$ . During the experiments the highest maximum temperature of the collector plate is  $115.7^\circ\text{C}$ , it is captured at Day 4. On the other hand, the lowest is  $101.7^\circ\text{C}$ , it is captured at Day 1. The maximum temperature of the collector plate at Day 2, Day 3, and Day 5 are  $112.9^\circ\text{C}$ ,  $102.2^\circ\text{C}$ , and  $107.1^\circ\text{C}$ , respectively. In order to make a better analysis, the temperature of the plate during experiments are

averaged. The average temperatures of the plate of solar collector during experiment at Day 1 and Day 2 are  $73.3^\circ\text{C}$  and  $87.3^\circ\text{C}$ , respectively. Furthermore, the average temperatures at Day 3, Day 4, and Day 5 are  $77.4^\circ\text{C}$ ,  $84.4^\circ\text{C}$ , and  $85.5^\circ\text{C}$ , respectively. Considering the solar energy radiation during experiment, shown in Table 1, these facts suggest that the higher solar energy radiation results in a higher temperature on the collector plate. The low solar energy radiation results in low temperature on the collector plate. The solar energy radiation on the plate at Day 2, Day 4, and Day 5 are above  $39 \text{ MJ}$ . These result in average temperature on the pate more than  $80^\circ\text{C}$ . In contrast, the average temperature on the collector plate at Day 1 and Day 3 is lower than  $80^\circ\text{C}$ . This is because the solar energy radiation on the plate collector is lower than  $39 \text{ MJ}$ .

The solar collector collects solar energy and it is used to heat the transfer fluid before it sent to the evaporator. Figure 3 also shows the temperature of the transfer fluid entering and leaving from the solar collector. It can be seen that the temperature of the fluid leaving from the collector is higher than temperature of the fluid entering the collector. In the first day, shown by Figure 3a, the average temperature of the transfer fluid entering and leaving from the solar collector are  $50.4^\circ\text{C}$  and  $60.8^\circ\text{C}$ , respectively. This suggests that the solar collector successfully heats the transfer fluid in order of  $10.4^\circ\text{C}$ . In the second day of experiment the average temperature of the transfer fluid entering and leaving from the solar collector are  $60.0^\circ\text{C}$  and  $82.7^\circ\text{C}$ , respectively. This fact reveals that the solar collector heats the transfer fluid in order of  $22.7^\circ\text{C}$ . In the fourth day of experiments the solar collector heats the transfer fluid from the average temperature of  $60.1^\circ\text{C}$  to  $81.6^\circ\text{C}$ . This reveals that the increasing average temperature is  $21.5^\circ\text{C}$ . While in the fifth day of experiment, the average temperature of the transfer fluid at the inlet and outlet of the solar collector are  $61.2^\circ\text{C}$  and  $83.1^\circ\text{C}$ , respectively. In other words, the temperature difference of the transfer fluid entering and leaving the solar collector is  $21.9^\circ\text{C}$ . In the third day of experiment, the graph is not shown in the figure, the average temperature of the transfer fluid when entering the solar collector and leaving the solar collector are  $59.4^\circ\text{C}$  and  $75.4^\circ\text{C}$ , respectively. Thus, the average temperature difference is  $16^\circ\text{C}$ . These facts reveal that the highest temperature difference of the transfer fluid resulted by the solar collector is  $22.7^\circ\text{C}$  (Day 4) and followed by  $21.9^\circ\text{C}$  (Day 5) and  $21.5^\circ\text{C}$  (Day 2). On the other hand, the lowest is  $10.4^\circ\text{C}$  (Day 1) and followed by  $16^\circ\text{C}$  (Day 3). This fact is comparable to the solar energy radiation discussed in Table 1.

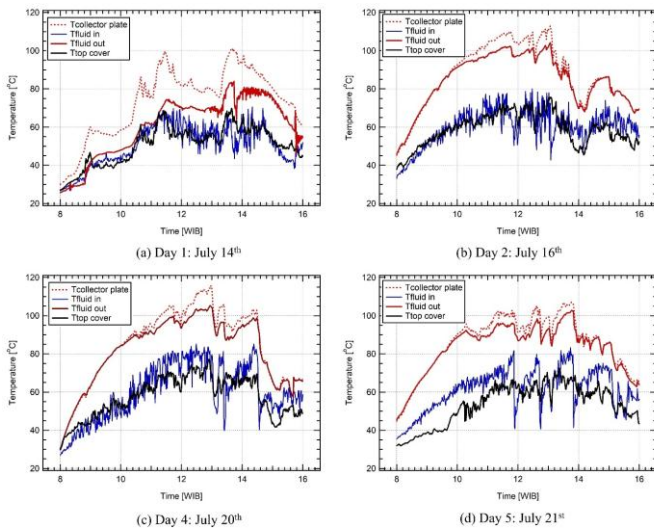


Fig. 3. Temperature of the solar collector during experiments

Figure 4 shows the heat loss from the solar collector during experiments. In the figure, only four days of experiments are presented. It can be seen that all graphs reveal the similar trend with the temperature of plate of the solar collector, as shown in Figure 3. The high temperature of the plate results in high heat loss. This is because the heat loss comparable to the temperature difference of collector plate and ambient. The figure suggests that the highest heat loss from the collector is from the top cover of the collector. The heat loss from the top cover is around 70% to 85% of the total heat loss. In the present solar collector, the top part of the collector is made of a double glass cover with a distance of 5 cm. It is suggested to further examine the effectiveness of the top cover in reducing the heat loss to the surrounding.

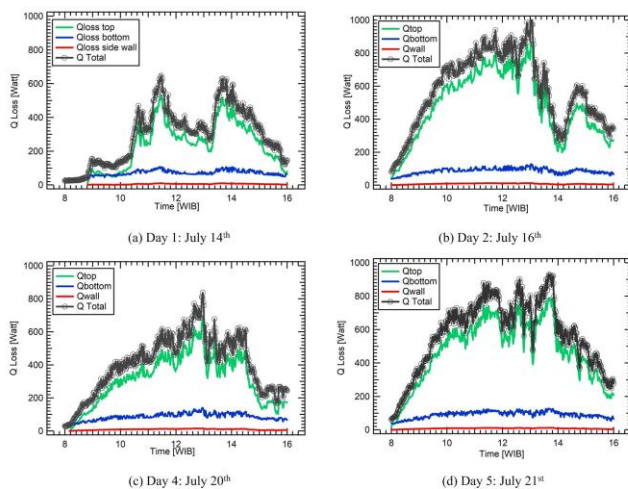


Fig. 4. Heat loss from the solar collector during experiments

### 1.3 Evaporator

Figure 5 shows temperature of the evaporator during experiments. The evaporator temperature is represented by wall temperature and the bottom temperature. In addition,

temperatures of the transfer fluid entering and leaving the evaporator are also shown. The seawater temperature which is resulted from numerical analysis is shown in the figure by solid black line. It can be seen in the figure that temperature of the seawater inside the evaporator is between the temperature of the evaporator wall and the temperature of the transfer fluid. And it strongly affected by temperature of the transfer fluid entering the evaporator. This is because the seawater is heated by the transfer fluid. The figure shows that all temperatures increase as time increases. However, after 14.00 WIB the temperatures decrease as time increases. This is because the temperature of the transfer fluid decreases as solar irradiance decreases. As a note, the driving force of evaporation rate consists of the temperature of seawater inside the evaporator and temperature of the condenser. The production rate of the solar desalination is affected by seawater temperature. The figure shows that the seawater temperature in the evaporator increase gradually from its lower value in the beginning of experiment. The transfer fluid brings solar energy from solar collector and releases the energy into the seawater. This fact suggests that the solar collector successfully collect the solar energy and transferring it into the seawater inside the evaporator. Since the temperature of the seawater increases, the evaporation will occur.

To perform the analysis, the temperature history of the evaporator is averaged and the results are presented in Table 2. In the table, the average temperatures of the transfer fluid entering and leaving the evaporator also the temperature difference are shown. In addition, the average temperatures on the bottom, sidewall, and seawater are also shown. It can be seen that the average temperature of the transfer fluid entering and leaving the evaporator vary from  $60.64^{\circ}\text{C}$  to  $70.62^{\circ}\text{C}$  and from  $39.02^{\circ}\text{C}$  to  $44.68^{\circ}\text{C}$ , respectively. The average temperature difference of the transfer fluid varies from  $21.61^{\circ}\text{C}$  to  $25.93^{\circ}\text{C}$ . This temperature difference shows the amount of the energy released in the evaporator to perform desalination. The lowest temperature difference of the transfer fluid is shown by Day 1, it is only  $21.6^{\circ}\text{C}$ . This is because the solar energy radiation during the first day of experiment is very low. According to Table 1, the solar energy in the first day of experiment is 26.40 MJ or it is the lowest in comparison with other days of experiments. On the other hand, the highest solar radiation is captured in the Day 4. As a result, the maximum temperature difference in the evaporator is also shown by Day 4, it is  $25.80^{\circ}\text{C}$ . In addition, the highest and the lowest average seawater temperatures in the evaporator are  $53.15^{\circ}\text{C}$  (Day 1) and  $54.92^{\circ}\text{C}$  (Day 4), respectively. This fact suggests that solar irradiance strongly affect the temperature of the seawater inside the evaporator.

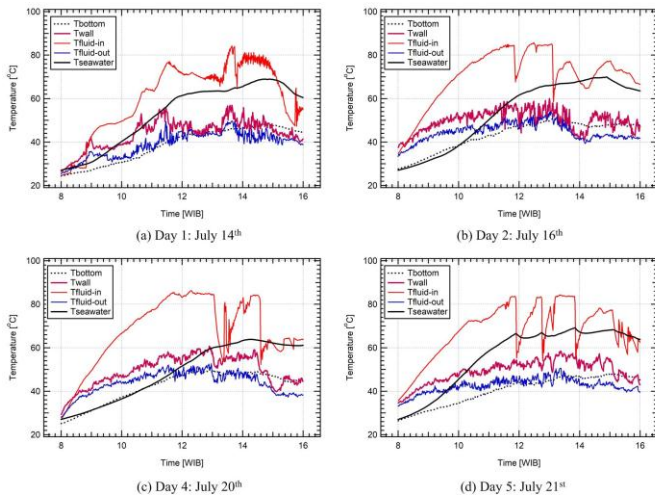


Fig. 5. Temperature of the evaporator during experiments

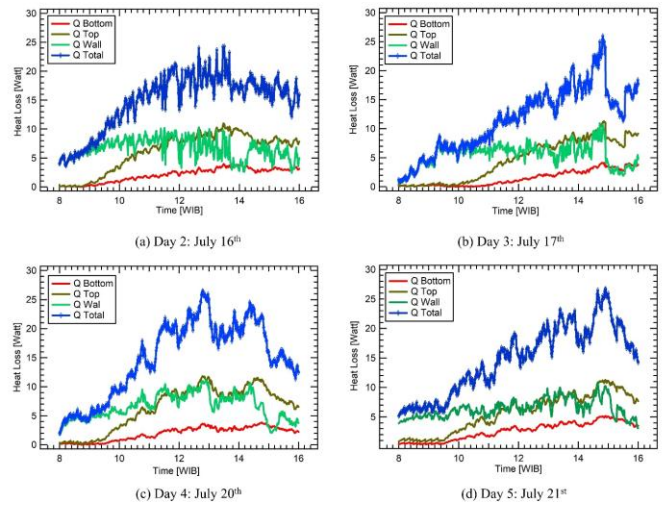


Fig. 6. Heat Loss from the evaporator during experiments

Table 2 Average temperature of the evaporator

Exper iment	Temperature Transfer fluid			Temperature of the evaporator		
	In	Out	Difference	Bottom	Side Wall	Seawater
Day 1	60.64 <sup>0</sup> C	39.02 <sup>0</sup> C	21.61 <sup>0</sup> C	38.80 <sup>0</sup> C	43.83 <sup>0</sup> C	53.15 <sup>0</sup> C
Day 2	70.02 <sup>0</sup> C	44.68 <sup>0</sup> C	25.33 <sup>0</sup> C	43.17 <sup>0</sup> C	49.93 <sup>0</sup> C	53.70 <sup>0</sup> C
Day 3	63.75 <sup>0</sup> C	40.57 <sup>0</sup> C	23.17 <sup>0</sup> C	38.53 <sup>0</sup> C	45.43 <sup>0</sup> C	53.70 <sup>0</sup> C
Day 4	69.75 <sup>0</sup> C	43.95 <sup>0</sup> C	25.80 <sup>0</sup> C	42.17 <sup>0</sup> C	49.41 <sup>0</sup> C	54.92 <sup>0</sup> C
Day 5	68.06 <sup>0</sup> C	42.54 <sup>0</sup> C	25.53 <sup>0</sup> C	40.48 <sup>0</sup> C	49.15 <sup>0</sup> C	56.23 <sup>0</sup> C

The average temperature of the seawater in the evaporator is higher than ambient temperature. Since the temperature of the evaporator is higher than ambient, some heat will also release to ambient as heat loss. In addition, the energy for evaporation is also drawn from the seawater. Thus, the heat capacity of the seawater will decrease to provide energy for evaporation and heat loss to the ambient. The heat loss from evaporator to the ambient is shown in Figure 6. The figure shows that the rate of heat loss from the top, bottom, and sidewall of the evaporator are almost similar. It can be seen that the rate of heat loss increases with increasing time. However, after 14.00 WIB, it decreases with increasing time. This is because, the solar irradiance decrease and temperature of the evaporator decrease significantly due to high evaporation rate.

### 1.4 Condenser

The vapor resulted by evaporation process will flow into the condenser. In the condenser it will be condensed on the condenser wall and results in fresh water. The rate of the condensation is affected by the temperature of the condenser wall. Figure 7 shows temperature history of the wall temperature, fin temperature of the condenser, and ambient temperature during the experiments. The figure shows that the maximum temperature on the condenser wall can reaching a value over than 45°C, except during Day 1. Temperature of the condenser is relatively higher than ambient temperature. This suggests that the ambient air can cool the condenser and absorb the heat of condensation. In other words, the condensation energy from the vapor is absorbed by the ambient air.

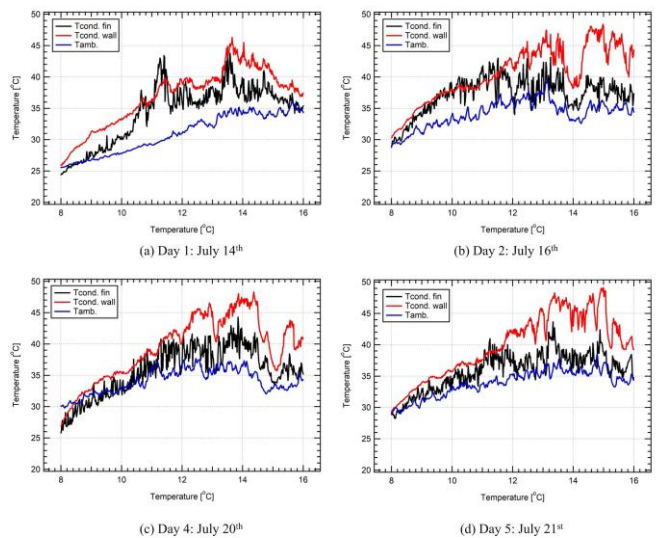


Fig. 7. Temperature of the condenser during experiments

### 1.5 Fresh water Production rate

The main objective of the natural vacuum solar desalination to produce fresh water from the seawater. Figure 8 shows the history of fresh water production rate during experiments. In the figure the solar irradiance is also shown. The figure shows that the production of fresh water starting at around 10.00 WIB and it depends of the solar irradiation. In the first day of experiment it starts at 10.00 WIB, but in the second day it starts earlier, it is at 9.36 WIB. This is because the solar irradiance in the first day is higher than in the second day of experiment. After this, during 10.00 WIB to 12.00 WIB, the fresh water production rate increases significantly. This is because temperature of the evaporator increases significantly. This fact reveals that during this time production rate is mainly forced by temperature of the seawater. During 12.00 WIB to 14.00 WIB, the production rate tends to be constant. This is because the solar irradiance is high but the ambient temperature is also high, reaching its maximum value. Furthermore, during 14.00 WIB to 15.00 WIB, the solar irradiance is still high but ambient temperature start to decrease. Here, the fresh water production rate increases with increasing time. This is because the production rate is mainly driven by the low ambient temperature. It makes the temperature in the condenser wall lower and at the same time there is sufficient heat in the evaporator. After 15.00 WIB, ambient temperature decreases with time. However, the production rate also decreases. This is because solar irradiance also decreases significantly. This makes no enough energy can be provided by solar collector to overcome the heat evaporation.

The above facts reveal that the characteristics of fresh water production rate can be divided into five different periods. The first period is initial period or the period without fresh water production. Typically, it is from the beginning until 10.00 WIB. Here, temperature of the evaporator is below the saturation temperature of the seawater. The second period is named as first rising rate. It is typically from 10.00 WIB to 12.00 WIB. In this period the main driving force for desalination is temperature of the seawater in the evaporator. The third period is named as constant production rate, typically from 12.00 WIB to 14.00 WIB. The fourth period is named as second rising production rate, typically from 14.00 WIB to 15.00 WIB. In this period the main driving force for desalination is ambient temperature. And the final period is falling production rate. Here the solar irradiance can't provide sufficient energy for evaporation process. During these experiments, these periods strongly affected by weather conditions.

The total fresh water production for all experiments are presented in Table 3. In the table the total fresh water production resulted from experiment and numerical are presented. In order to provide discussion, the average ambient temperature and total solar radiation for all experiments are also shown. It can be seen that the numerical and experimental results show a good agreement. The maximum discrepancy is only 9.99%. This fact reveals that numerical method predicts the fresh water production well. The results show that the fresh water production varies from 0.87 liters to 1.47 liters. It

depends of the ambient temperature and total solar irradiation. The lowest total solar radiation is collected in the first day of experiment. Here, the lowest fresh water production is also captured. It is only 0.89 liters. The highest fresh water production is 1.47 liter and captured in the fourth day of experiment. In this experiment the total solar energy collected in the collector is 39.84 MJ. The total solar energy radiation in Day 2, Day 4, and Day 5 of experiments are almost similar. However, the total fresh water productions are different. This is because the ambient temperatures are also different. The higher ambient temperature result in the lower fresh water production. This fact confirms that the fresh water production of the natural vacuum solar desalination affected by seawater temperature in the evaporator and ambient temperature.

Table III  
Fresh water production and Thermal efficiency

Experi ment	Ambient		Fresh water production [Litre]			Thermal Efficien cy
	Ave. Temp. [°C]	Total Radiati on [MJ]	Exp .	Nu m.	Discrep ancy	
Day 1	30.617	26.40	0.89	0.8	9.91%	7.94%
Day 2	32.585	39.72	1.27	1.2	5.67%	7.53%
Day 3	31.968	36.93	1.09	1.0	7.94%	6.95%
Day 4	31.495	39.84	1.47	1.4	4.51%	8.69%
Day 5	33.310	39.33	1.21	1.3	9.99%	7.24%

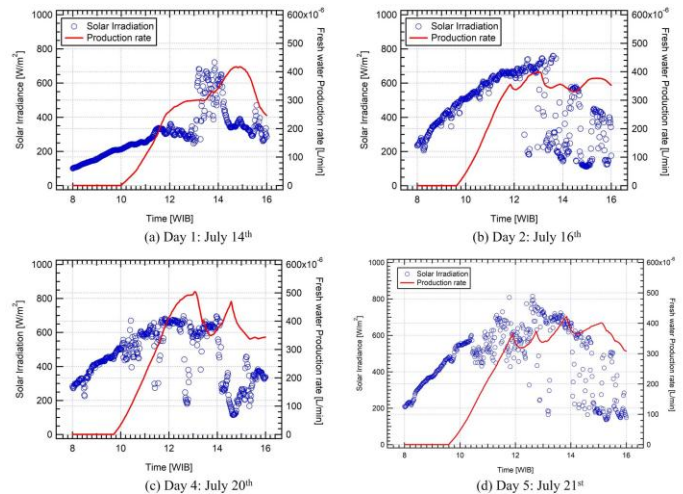


Fig. 8. Fresh water production rate during experiments

In order to examine the energy utilization of the present prototype of natural vacuum solar desalination, thermal efficiency of the system has been calculated by using equation (30). Thermal efficiency of the system during experiments is shown in the last column of Table 3. Data of the table shows that thermal efficiency of the system varies between 6.95% and 8.69%. The thermal efficiency of the present natural vacuum is very low. The results also show that there is no

strong correlation of solar irradiation and thermal efficiency of the system.

Several researchers have carried out studies on the natural vacuum solar desalinations. In order to provide comparisons, results of the previous studies were presented in Table 4. The maximum total fresh water production of the present result was also presented in the table. The result of the present study is lower than previous studies. As a note, in the present study the solar collector area is 3 m<sup>2</sup>. The fresh water production varies between 2.05 liter per m<sup>2</sup> in collector day [20] and 5.5 liter per m<sup>2</sup> in collector per day [16]. In those studies, however, the fresh water production resulted from numerical method instead of experimental one. This fact suggests that the present result is very low in comparison with those previous results. Therefore, several modifications are needed to improve the performance of the system. Overall, it can be seen that the highest water production of 100 l per day of Gude et al, used a solar collector with a size of 18m<sup>2</sup>, followed by a maximum of 2 with a production of 5.54 l per day of water used Maroo's at al 1m<sup>2</sup> solar collector. The third highest of the research results that have been carried out experimentally using 3m<sup>2</sup> solar collectors were less than optimal because of the low intensity of the sun as shown in Figure 2. The calculation is higher than experimental because the weather is unpredictable, depending on the thickness of the cloud blocking, able to be penetrated by the sun or not, followed by No. 4 with the results of 1.2 l per day of water production that Ambarita has examined using an electric heater is considered not optimal because it has to pay electricity to run. Clean water production number 5 is 0.41 l per day using a solar collector with a size of 0.2 m<sup>2</sup> research from Al-Kharabsheh et al. [14].

Table IV  
Result comparison with previous researches

No	Researcher	Heat Source	Method	Fresh Water Production
1	Gude et al. (2012)	Solar Collector [ 18 M <sup>2</sup> ]	Analytical	100 L/day
2	Maroo et al. (2009)	Solar Collector [ 1 M <sup>2</sup> ]	Analytical	5.54 L/day
3	Al-Kharabsheh et al. (2003)	Solar Collector [ 0.2 M <sup>2</sup> ]	Analytical	0.41 L/day
4	Ambarita (2016)	Electric heater	Experimental	1.2 L/day
5	The present work	Solar Collector [ 3 M <sup>2</sup> ]	Experimental & Numerical	1.4 L/day

#### IV. CONCLUSIONS

In this study, a prototype of natural vacuum solar desalination consists of solar collector, evaporator and condenser as the main components has been designed and

fabricated. The prototype is tested by exposing it to solar irradiance on a top roof of a building at Medan city of Indonesia for five days. The experiments are carried out from 8.00 WIB to 16.00 WIB local time. The conclusions of the present study are explained as following. The solar collector successfully collects the solar energy and transfer it into the seawater in the evaporator. The maximum temperature on the collector plate varies between 101.7°C and 115.7°C. The average temperature of the seawater in the evaporator varies between 53.15°C and 54.92°C. The characteristics of fresh water production rate can be divided into five different periods. The first period is initial period or the period without fresh water production. Typically, it is from the beginning until 10.00 WIB. Here, temperature of the evaporator is below the saturation temperature of the seawater. The second period is named as first rising rate. It is typically from 10.00 WIB to 12.00 WIB. In this period the main driving force for desalination is temperature of the seawater in the evaporator. The third period is named as constant production rate, typically from 12.00 WIB to 14.00 WIB. The fourth period is named as second rising production rate, typically from 14.00 WIB to 15.00 WIB. In this period the main driving force for desalination is ambient temperature. And the final period is falling production rate. The results show that the fresh water production varies from 0.87 liters to 1.47 liters. It depends of the ambient temperature and total solar irradiation. Thermal efficiency of the present system varies between 6.95% and 8.69%. This fact suggests that the performance of the present system is very low. Thus, several modifications are needed to improve the performance of the system.

#### REFERENCES

- [1]. Sharon, H., and Reddy, K. S., 2015. A review of solar energy driven desalination technologies, *Renewable and Sustainable Energy Reviews* 41, 1080-1118.
- [2]. Eltawil, M. A., Zhengming, Z., and Yuan, L., 2009. A review of renewable technologies integrated with desalination systems, *Renewable Sustainable Energy Reviews* 13, 2245-62.
- [3]. Kalogirou, S., 2005. Seawater desalination using renewable energy sources. *Prog Energy Combust Sci* 31, 242-81.
- [4]. Subramani, A., Badruzzaman, M., Oppenheimer, J., and Jacangelo, J.G., 2011. Energy minimization strategies and renewable energy utilization for desalination: a review, *Water Res* 45, 1907-20.
- [5]. Gude, V. G., Nirmalakhadan, N., Deng, S., and Maganti, A., 2012. Feasibility study of a new two-stage low temperature desalination process, *Energy Conversion and Management* 56, 192-198.
- [6]. Li, C., Goswami, D.Y., Shapiro, A., Stefanakos, E.K., and Demirkaya, G., 2012. A new combined power and desalination system driven by low grade heat for concentrated brine, *Energy* 46, 582-595.
- [7]. Araghi, A. H., Khiadani, M., and Hooman, K., 2016. A novel vacuum discharge thermal energy combined desalination and power generation system utilizing R290/R600a, *Energy* 98,215-224.
- [8]. Gao, W., Wang, D., Xu, C., and Li, C., 2016. Experimental study on water separation process in a novel spray flash vacuum evaporator with heat-pipe, *Desalination* 386, 39-47.
- [9]. Dow, N., Gray, S., Li, J., Zhang, J., Ostarcevic, E., Liubinas, A., Atherton, P., Roeszler, G., Gibbs, A., and Duke M., 2016. Pilot trial of membrane distillation driven by low grade waste heat: Membrane fouling and energy assessment, *Desalination* 391, 30-42.
- [10]. Christ, A., Regenauer-Lieb, K., and Chua, H., 2015. Boosted Multi-Effect Distillation for sensible low-grade heat sources: A comparison with feed pre-heating Multi-Effect Distillation, *Desalination* 366, 32-46.

- [11]. Gude, V. G., 2015. Energy storage for desalination process powered by renewable energy and waste heat sources, *Applied energy* 137, 877-898.
- [12]. Bundschuh, J., Ghaffour, N., Mahmoudi, H., Goosen, M., Mushtaq, S., and Hoinkis, J., 2015. Low cost low-enthalpy geothermal heat for fresh water production: Innovative applications using thermal desalination process, *Renewable and Sustainable Energy Reviews* 43, 196-206.
- [13]. Cioccolanti, L., Savoretti, A., Renzi, M., Caresana, F., and Comodi, G., 2016. Comparison different operation modes of a single effect thermal desalination plant using waste heat from m-CHP unit, *Applied Thermal Engineering* 100, 646-657.
- [14]. Al-Kharabsheh, S. and Goswami, D.Y., 2004. Theoretical analysis of a water desalination system using low grade solar heat, *Journal of Solar Energy Engineering* 126, 774-780.
- [15]. Gude, V. G., and Nirmalakandan, N., 2008. Combined desalination and solar-assisted air-conditioning system, *Energy Convers Manag* 49, 3326-30.
- [16]. Gude, V. G., Nirmalakandan, N., Deng, S., and Maganti, A., 2012. Low temperature desalination using solar collectors augmented by thermal energy storage, *Appl Energy* 91-1, 466-74.
- [17]. Ayhan, T. and Al-Madani, H., 2010. Feasibility study of renewable energy powered seawater desalination technology using natural vacuum technique, *Renewable Energy* 35, 506-14.
- [18]. Ambarita, H., 2017. Numerical study on natural vacuum solar desalination system with varying heat source temperature, *IOP Conf. Series: Materials Science and Engineering* 180, 012024.
- [19]. Setyawan, E. Y., Napitupulu, N. A., Siagian, P., and Ambarita, H., 2017. Field tests of a natural vacuum solar desalination system using hybrid solar collector, *IOP Conf. Series: Materials Science and Engineering* 237, 012012.
- [20]. Al-Kharabsheh, S. and Goswami, D.Y., 2003. Analysis of an innovative water desalination system using low-grade solar heat. *Desalination* 156, 323-32.
- [21]. Churchill, S. W., and Chu, H. H. S., 1975. Correlating Equations for Laminar and Turbulent Free Convection from a Vertical Plate, *Int. Journal of Heat and Mass Transfer* 18, 1323.
- [22]. Ambarita, H., 2016. Study on the performance of natural vacuum desalination system using low grade heat source, *Case Studies in Thermal Engineering* 8, 346-358.
- [23]. *Incropera, F. P., DeWitt, D. P., Bergman, T. L., and Lavine, A. S., 2006. Fundamentals of Heat and Mass Transfer, 6th Ed*
- [24]. Isdale, J. D., Spence, C. M., and Tudhope, J. S., 1972. Physical properties of sea water solutions: viscosity, *Desalination*, 10(4), 319-328.
- [25]. Jamieson, D. T., and Tudhope, J. S., 1970. Physical properties of sea water solutions – Thermal Conductivity, *Desalination*, 8, 393-401.
- [26]. Korosi, A., and Fabuss, B. M., 1968. Viscosity of liquid water from 25°C to 150°C, *J. Anal. Chem.*, 40, 157-162.
- [27]. Lloyd, J. R., and Sparrow, E. M., 1970. Combined Forced and Free Convection Flow on Vertical Surfaces, *International Journal of Heat Mass Transfer* 13, 434.
- [28]. Maroo, S. C., and Goswami, D. Y., 2009. Theoretical analysis of a single-stage and two-stage solar driven flash desalination system based on passive vacuum generation, *Desalination* 249, 635-46.
- [29]. Rohsenow, W. M., Hartnett, J. P., and Ganic, E. N., 1985. *Handbook of Heat Transfer*, third edition, Mc Graw-Hill Book Company, New York, pp. 6.31-6.41.
- [30]. Sharqawy, M. H., V Lienhard, J. H., and Zubair, S. M., 2010. Thermophysical properties of seawater: a review of existing correlation and data, *Desalination and Water Treatment* 16, 354-380.
- [31]. Bemporad, G., A., 1995. Basic Hydrodynamic Aspects of a Solar Energy Based Desalination Process, *Desalination* 54, 125-134.
- [32]. Bromley, L. A., Diamond, A.E., Salami, E., and Wilkins, D.G., 1970. Heat capacities and enthalpies of sea salt solutions to 200°C, *Journal of Chemical and Engineering Data*, 15, 246-253.